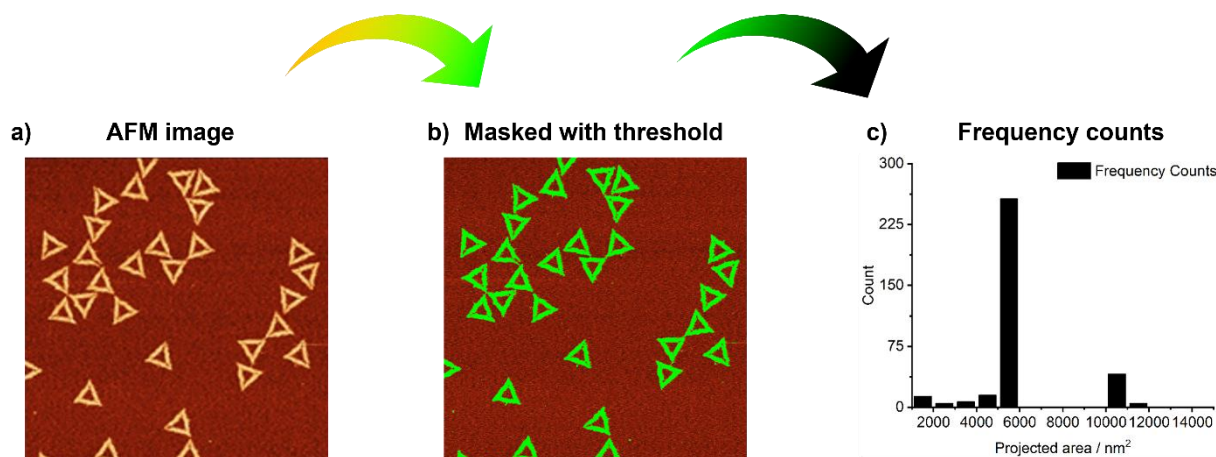


## Electronic Supplementary Material

# Superstructure-dependent stability of DNA origami nanostructures in the presence of chaotropic denaturants

Marcel Hanke, Daniel Dornbusch, Emilia Tomm, Guido Grundmeier, Karim Fahmy\* and Adrian Keller\*



**Figure S1.** Illustration of AFM image data processing and grain analysis. a) Each individual image was flattened and height adjusted. b) DNA origami triangles in the image were masked using an appropriate height threshold. c) The histogram of the projected surface area values of the masked DNA origami was determined for at least 3 images and evaluated in the projected surface area range from  $1 \times 10^3$  to  $15 \times 10^3$  nm<sup>2</sup> using a bin size of  $1 \times 10^3$  nm<sup>2</sup>, resulting in a total number of 14 bins.

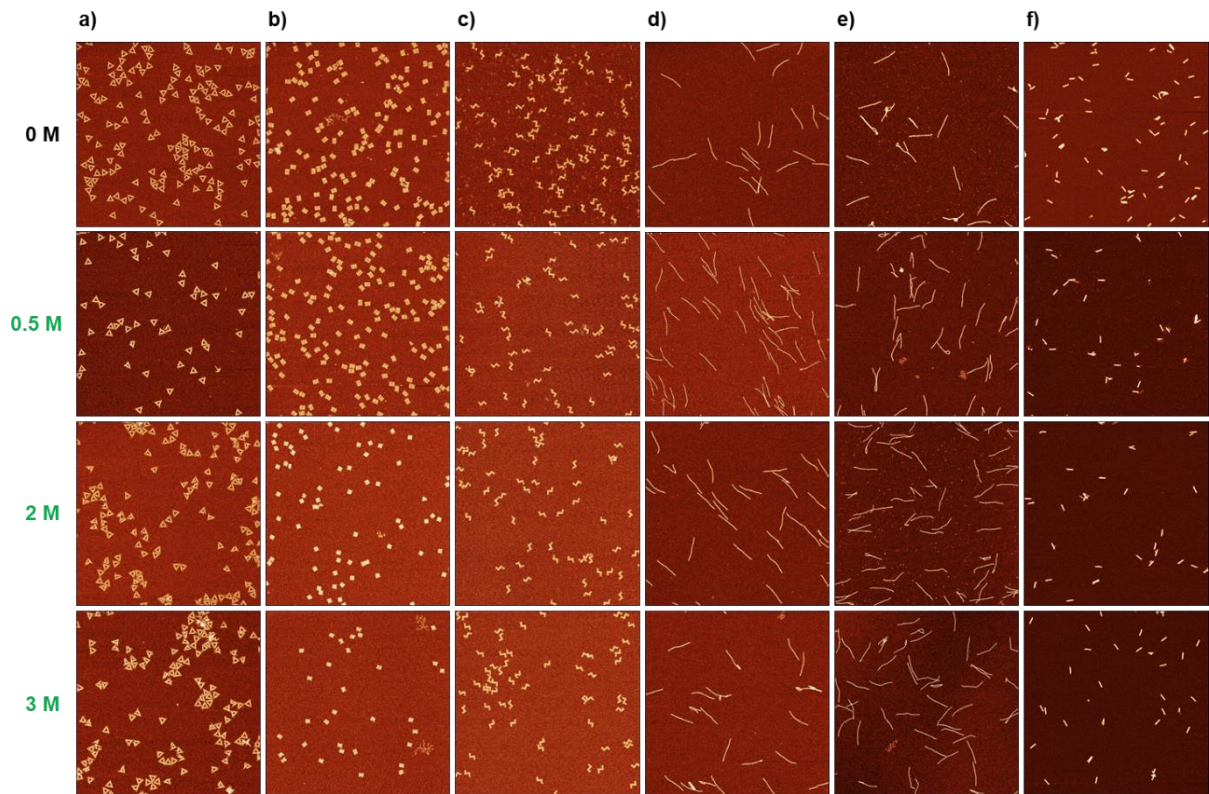


**Figure S2.** AFM images of DNA origami triangles (a), rectangles (b), Z shapes (c), 6HBs 42-bpCS (d), 6HBs 21-bpCS (e), and 24HBs (f) adsorbed on mica after incubation in different Gdm<sub>2</sub>SO<sub>4</sub> concentrations. The size of each AFM image is 3 x 3 μm<sup>2</sup> with a resolution of 1024 x 1024 px and a z-range of 3 nm (a-e) and 6 nm (f), respectively.

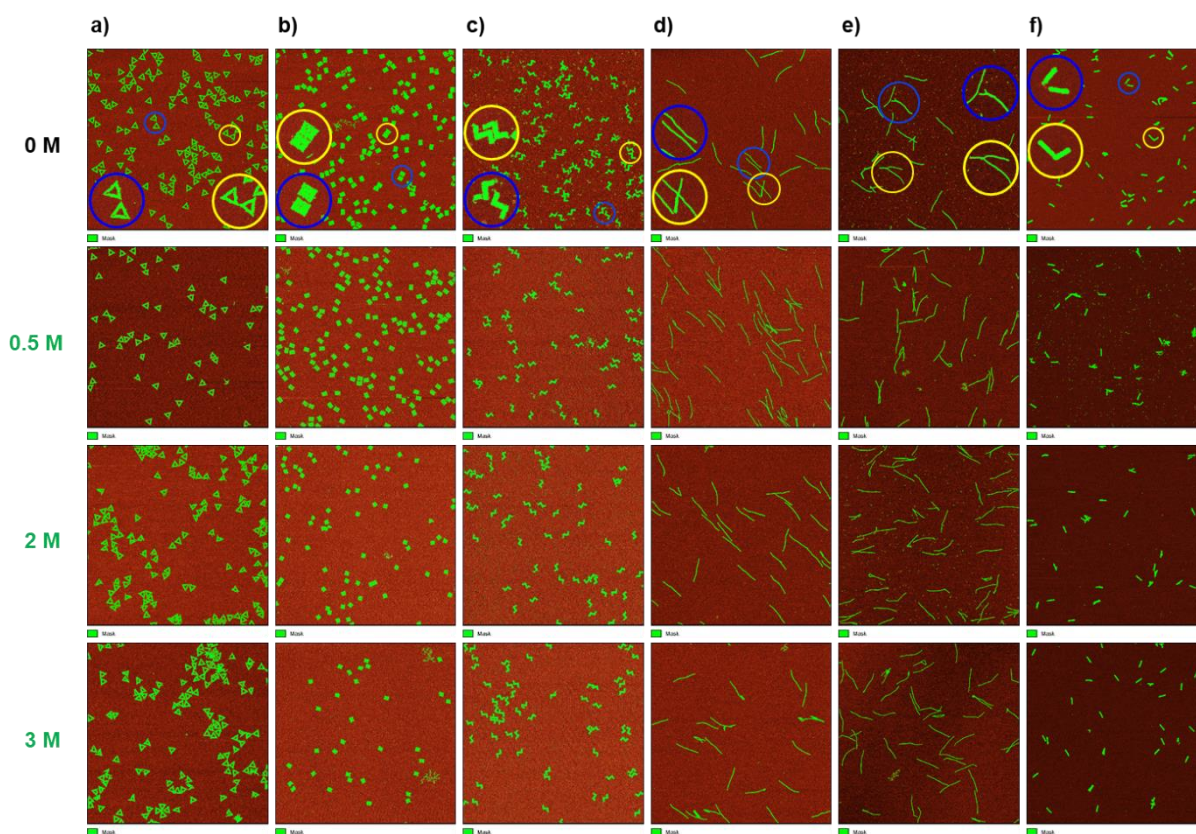


**Figure S3.** Masked AFM images of DNA origami triangles (a), rectangles (b), Z shapes (c), 6HBs 42-bpCS (d), 6HBs 21-bpCS (e), and 24HBs (f) adsorbed on mica after incubation in different Gdm<sub>2</sub>SO<sub>4</sub> concentrations. The masks are shown in green. The blue and yellow circles show DNA origami nanostructures that are identified as neighboring monomers and dimers, respectively.

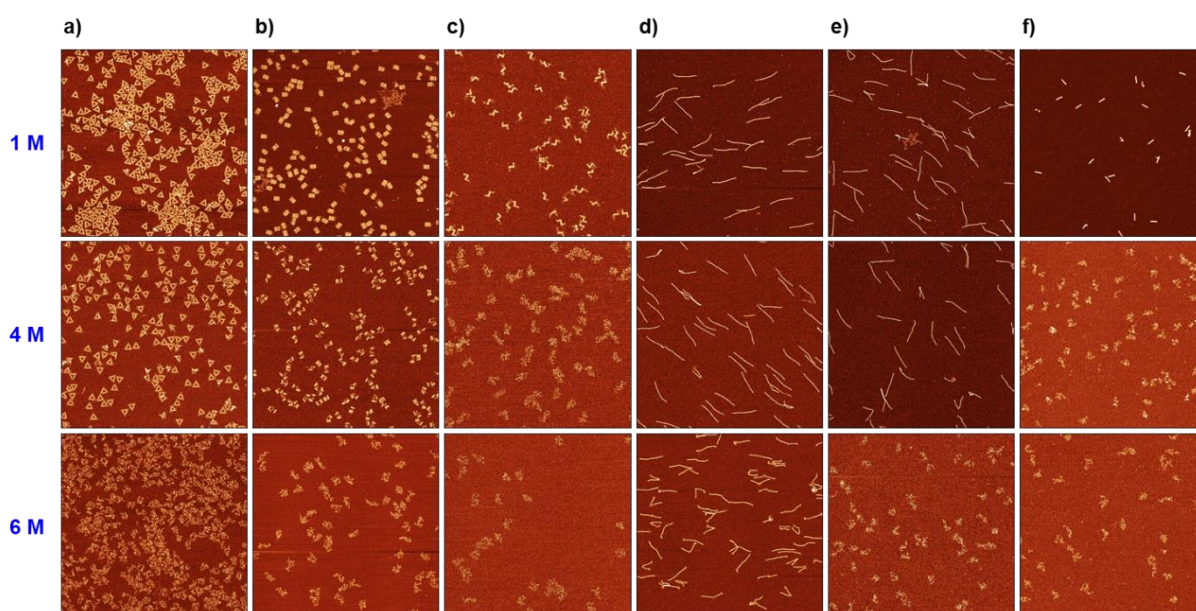


**Figure S4.** AFM images of DNA origami triangles (a), rectangles (b), Z shapes (c), 6HBs 42-bpCS (d), 6HBs 21-bpCS (e), and 24HBs (f) adsorbed on mica after incubation in different GdmCl concentrations. The size of each AFM image is  $3 \times 3 \mu\text{m}^2$  with a resolution of  $1024 \times 1024 \text{ px}$  and a z-range of 3 nm (a-e) and 6 nm (f), respectively. For the completely denatured DNA origami the z-range was reduced to 2 nm (b and e at 6 M) and 3 nm (f at 4 M and 6 M), respectively.

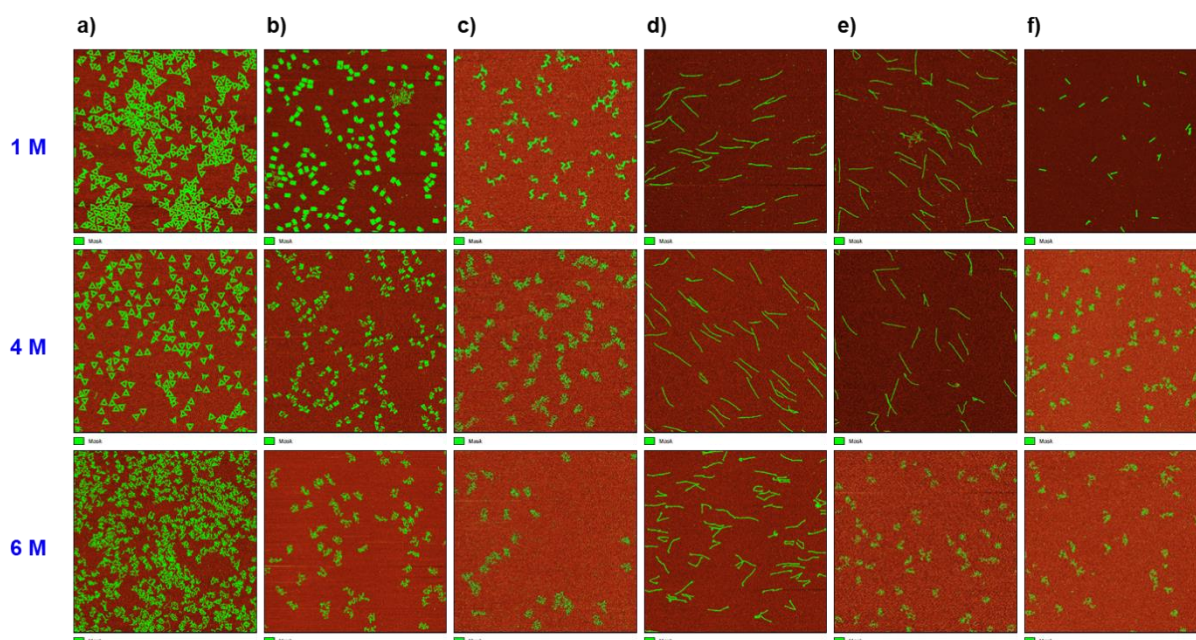


**Figure S5.** Masked AFM images of DNA origami triangles (a), rectangles (b), Z shapes (c), 6HBs 42-bpCS (d), 6HBs 21-bpCS (e), and 24HBs (f) adsorbed on mica after incubation in different GdmCl concentrations. The masks are shown in green.

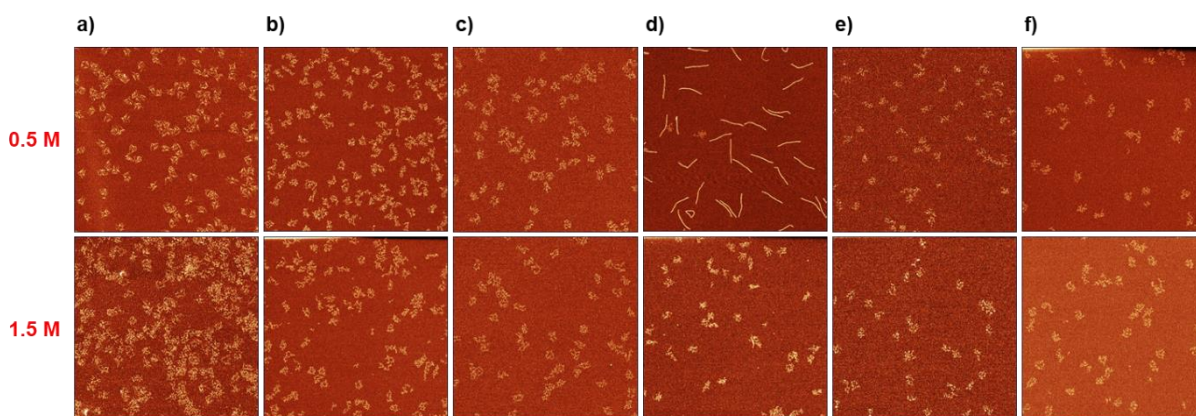


**Figure S6.** AFM images of DNA origami triangles (a), rectangles (b), Z shapes (c), 6HBs 42-bpCS (d), 6HBs 21-bpCS (e), and 24HBs (f) adsorbed on mica after incubation in different TPACl concentrations. The size of each AFM image is  $3 \times 3 \mu\text{m}^2$  with a resolution of  $1024 \times 1024 \text{ px}$  and a z-range of 3 nm (a-d,f). For the completely denatured DNA origami, the z-range was reduced to 2 nm (a and d at 1.5 M and e at 0.5 and 1.5 M).

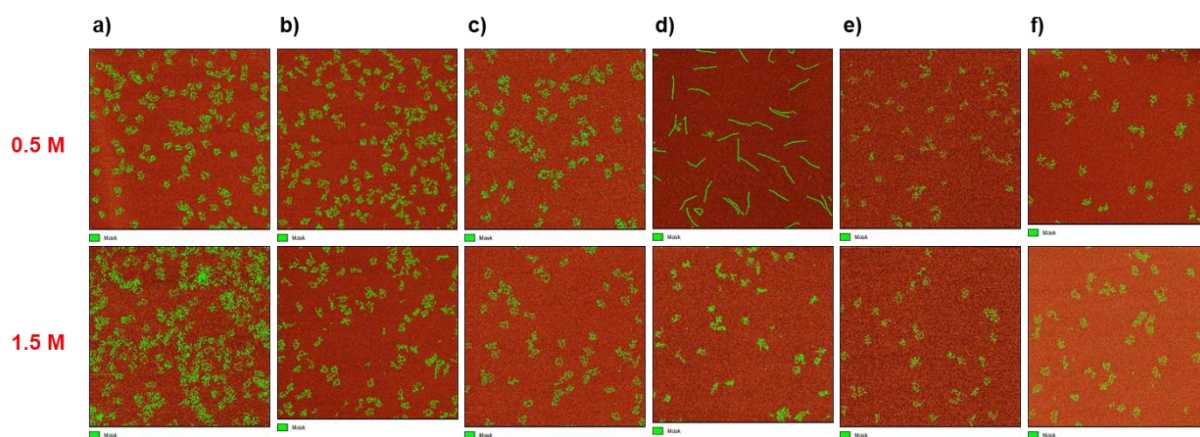


**Figure S7.** Masked AFM images of DNA origami triangles (a), rectangles (b), Z shapes (c), 6HBs 42-bpCS (d), 6HBs 21-bpCS (e), and 24HBs (f) adsorbed on mica after incubation in different TPACl concentrations. The masks are shown in green.

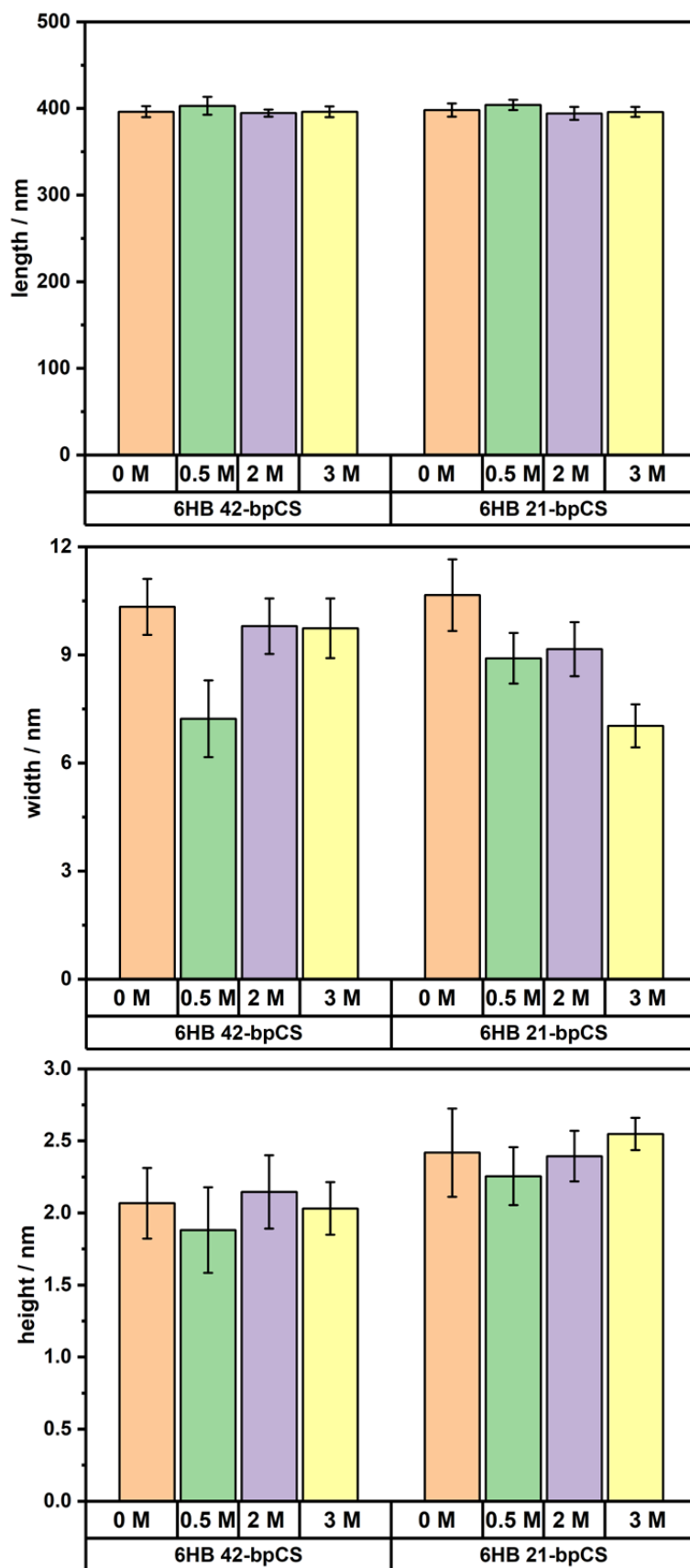


**Figure S8.** Average length, width, and height of the two different DNA origami 6HB designs after exposure to different concentrations of  $Gdm_2SO_4$ . The variations in 6HB width correlate well with the observed variations in the projected surface area in Figure 2. For each condition, 10 individual 6HBs have been analyzed.

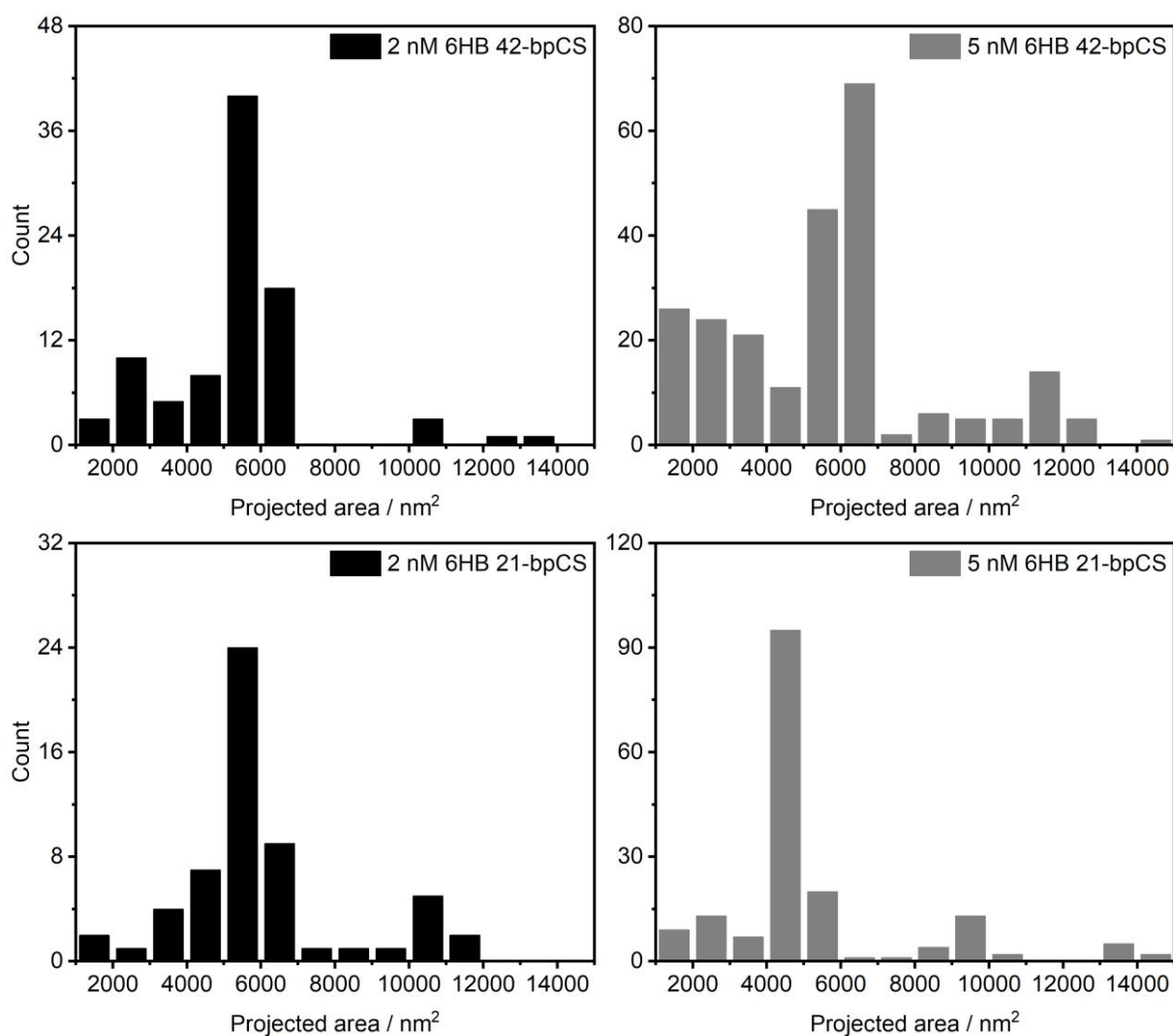


**Figure S9.** Projected surface area histograms of the two DNA origami 6HB designs at 2 nM and 5 nM concentrations in pure buffer without chaotropic salts. For the 42-bpCS design, the distribution is notably broadened at 5 nM due to the dense adsorption of 6HBs, which lie on top and cross each other. This effect is less pronounced for the 21-bpCS design, presumably because of its larger stiffness.

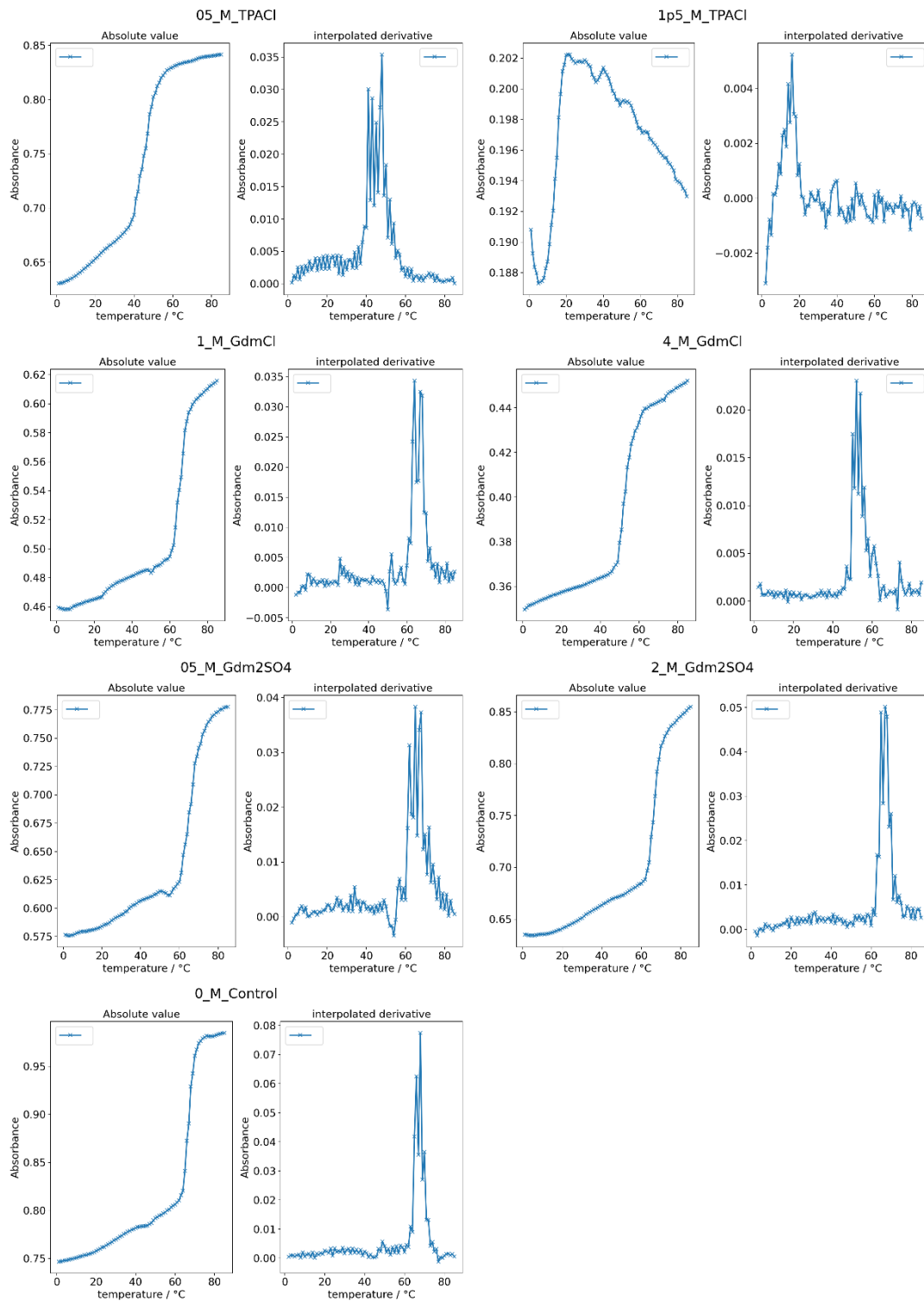


**Figure S10.** Absorption of 2D DNA origami triangles at 260 nm and its interpolated derivative measured from 1 °C to 85 °C at a rate of 0.5°C/min.



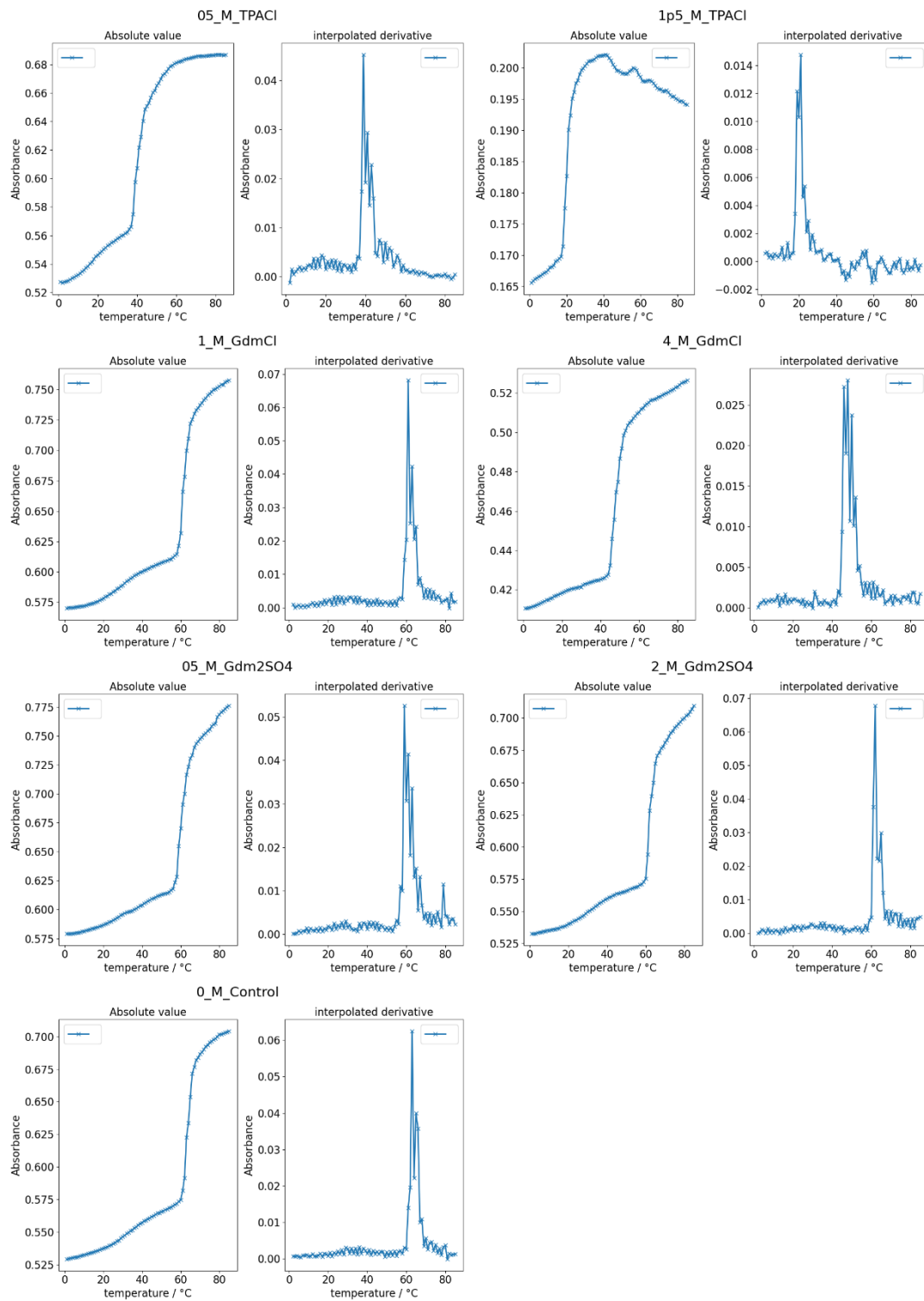


**Figure S11.** Absorption of 2D DNA origami rectangles at 260 nm and its interpolated derivative measured from 1 °C to 85 °C at a rate of 0.5°C/min.

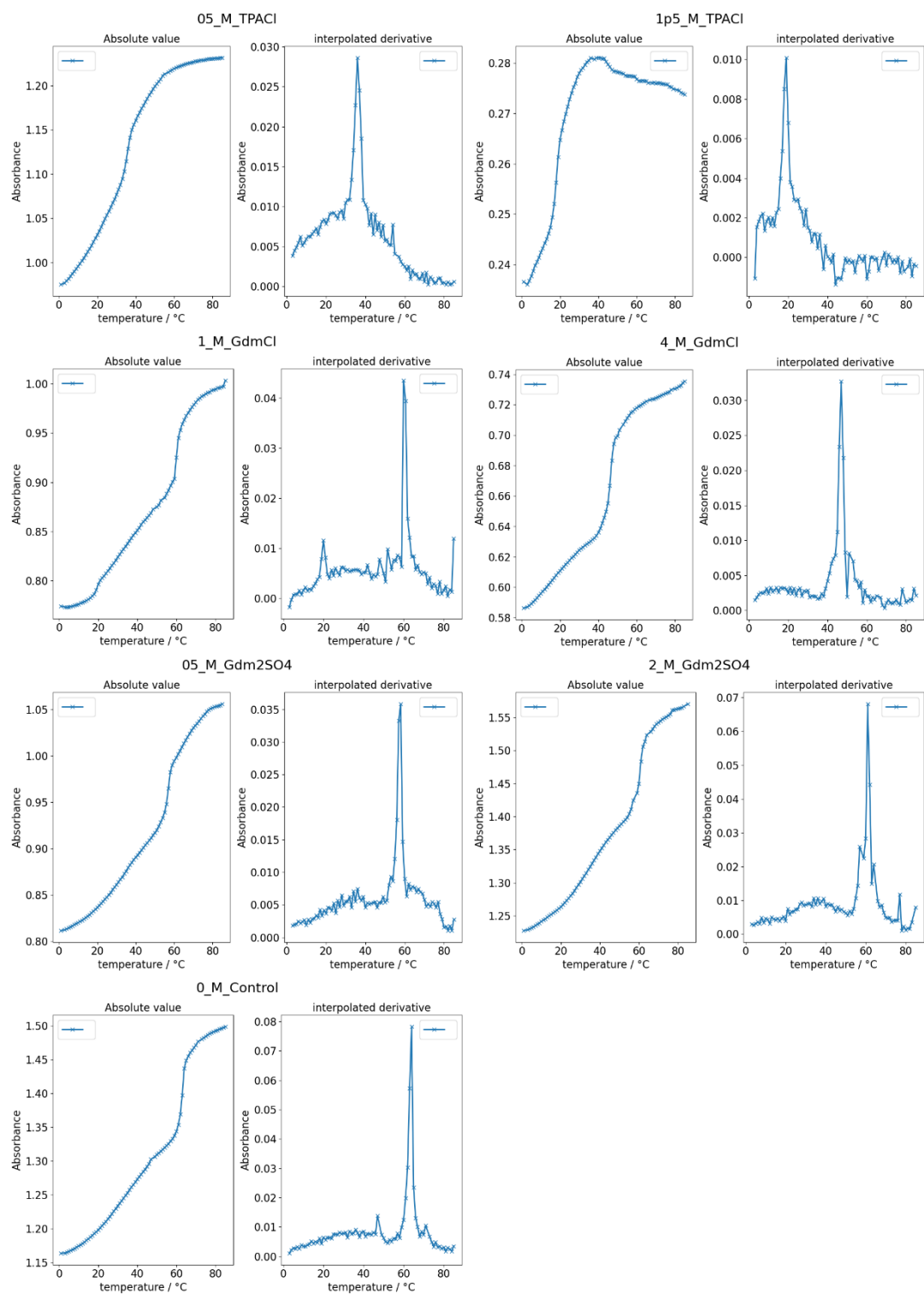


**Figure S12.** Absorption of 2D DNA origami Z shapes at 260 nm and its interpolated derivative measured from 1 °C to 95 °C at a rate of 0.5 °C/min

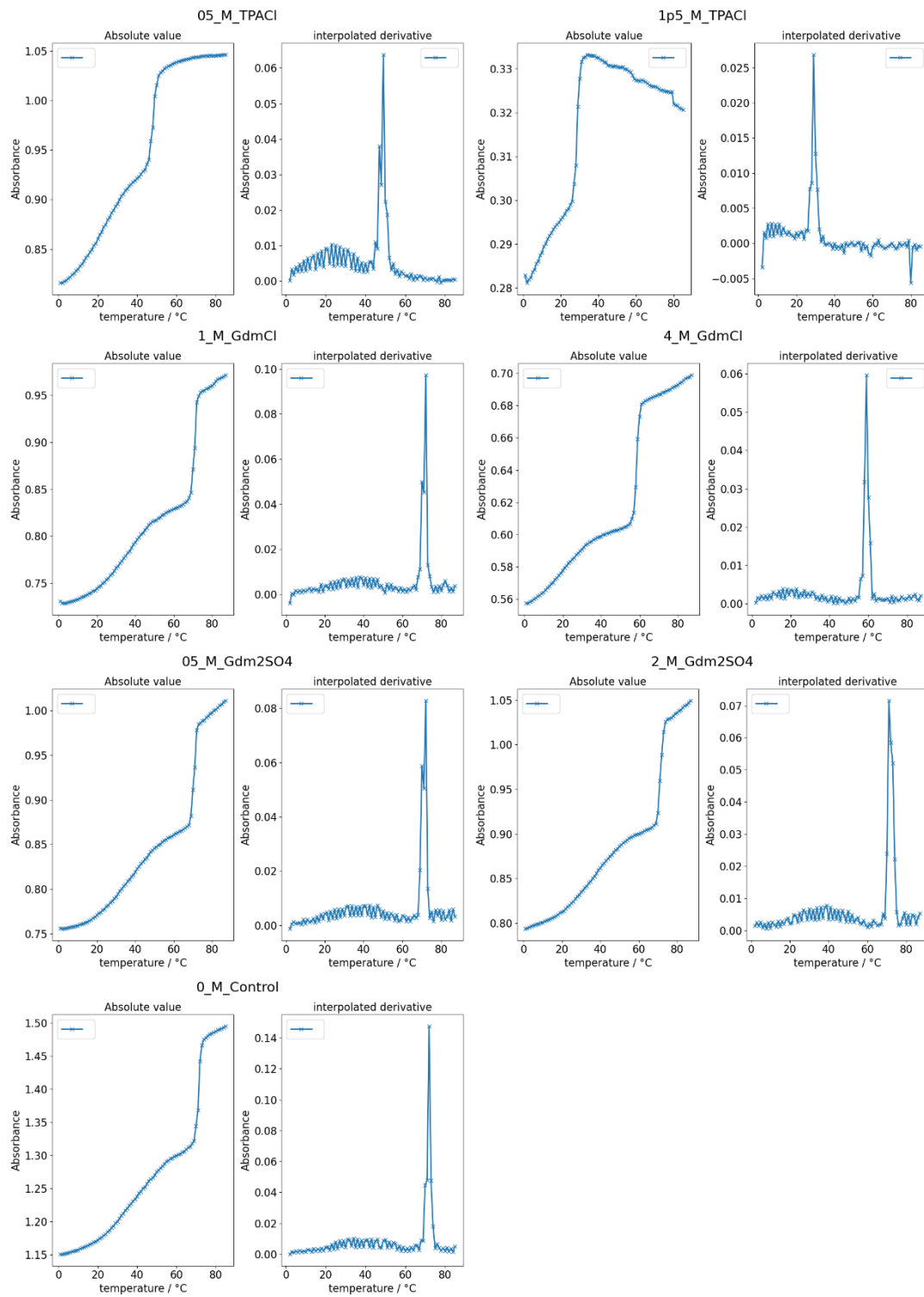


**Figure S13.** Absorption of 3D DNA origami 6HBs 42-bpCS at 260 nm and its interpolated derivative measured from 1 °C to 85 °C at a rate of 0.5 °C/min.

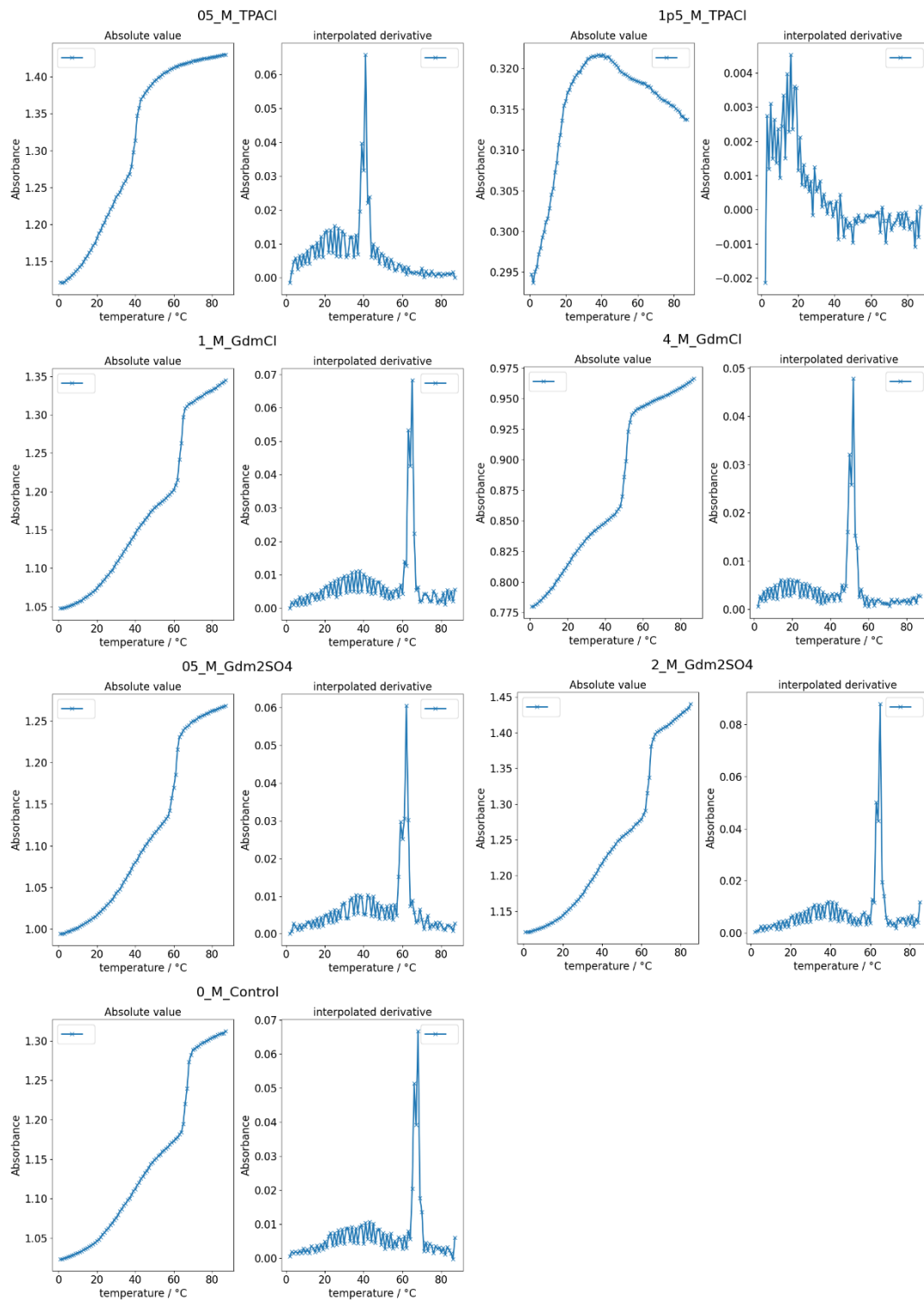


**Figure S14** Absorption of 3D DNA origami 6HBs 21-bpCS at 260 nm and its interpolated derivative measured from 1 °C to 85 °C at a rate of 0.5°C/min.

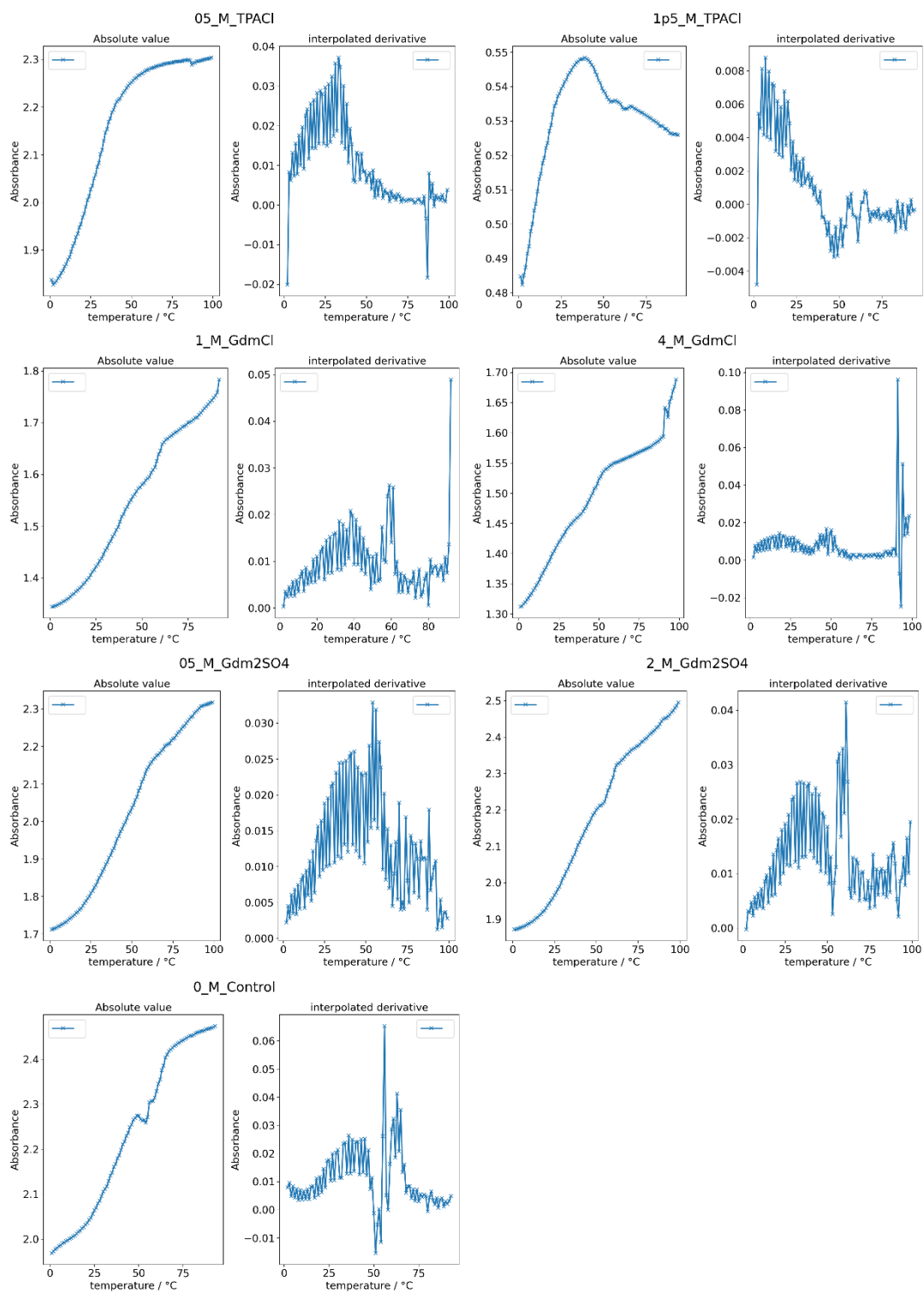


**Figure S15.** Absorption of 3D DNA origami 24HBs at 260 nm and its interpolated derivative measured from 1 °C to 95 °C at a rate of 0.5 °C/min.